ELSEVIER

Thermochimica Acta 280/281 (1996) 175–190

thermochimica acta

Use of phenomenological kinetics and the enthalpy versus temperature diagram (and its derivative — DTA) for a better understanding of transition processes in glasses[1]

Jaroslav Šesták

Institute of Physics, Division of Solid-State Physics, Academy of Sciences of the Czech Republic, Cukrovarnická 10, 16200 Praha 6, Czech Republic

Abstract

Thermophysical bases of vitrification and crystallization are discussed in terms of the enthalpy versus temperature diagram and its derivative (DTA) illustrating relaxation and glass transformation as well as crystallization of glassy and amorphous states to form stable and metastable phases. Non-isothermal kinetics are thoroughly discussed and the use of one- (JMAEK) and two- (SB) parameter equations is described. The practical case of the complementary $70SiO_2$–$10Al_2O_3$–$20ZnO$ glass treatment is demonstrated for both standard nucleation–growth curves and corresponding DTA recordings; these show a good coincidence of the activation energies obtained.

Keywords: Crystallization; DSC; DTA; Enthalpy–temperature diagram; Glass transitions; Non-isothermal kinetics; SiO_2–Al_2O_3–ZnO; Vitrification

1. Introduction

Second phase nucleation and its consequent growth can be understood as a general process of new phase formation. It touches almost all aspects of our universe accounting for the formation of smog as well as the embryology of viruses [1]. On the other hand the supression of nucleation is important for the general process of vitrification, itself important in such diverse fields as metaglasses or cryobiology trying to achieve

[1] Dedicated to Professor Hiroshi Suga.

SSDI 0040-6031(95)02641-X

non-crystallinity for highly non-glass-forming alloys or intra- and extracellular solutions needed for cryopreservation.

A characteristic process worthy of specific note is the sequence of relaxation–nucleation–growth processes associated with the transition of the non-crystalline state to the crystalline one. Such a process is always accompanied by a change of enthalpy content which, in all cases, is detectable by *thermometric* (differential thermal analysis, DTA) and/or *calorimetric* (differential scanning calorimetry, DSC) measurements [2,3]. Some essential aspects of such types of investigation will be reviewed and attempts will be made to explain them more simply.

The article has two parts with different information levels. The aim of Section 3 is to show an easy way of graphically illustrating processes associated with devitrification. The diagram of enthalpy versus temperature is employed, including its relationship to conventional DTA–DSC measurements; this is easily understandable in terms of the temperature derivatives [3]. Inherent information, however, is very complex and its successful utilization, particularly in determining the reaction kinetics of crystallization, is not easy. Therefore a more specialised section 4 is added in order to review some current practices of non-isothermal kinetics evaluations.

2. Theoretical basis of DTA–DSC

Most DTA instruments can be described in terms of a double non-stationary calorimeter [3] in which the thermal behaviour of the sample (S) is compared with that of an inert reference (R) material. The resulting effects produced by the change of the sample enthalpy content can be analysed at four different levels, namely:

(1) *identity* (fingerprinting of sequences of individual thermal effects);
(2) *quality* (determination of points characteristic of individual effects such as beginnings, onsets, outsets, inflections and apexes);
(3) *quantity* (areas, etc.);
(4) *kinetics* (dynamics of heat sink and/or generation responsible for the peak shapes).

The identity level plays an important role in deriving the enthalpy against temperature plots while study of kinetics pays attention to profile of their derivatives.

From the balance of thermal fluxes the DTA equation can be established [3,4] relating the measured quantity, i.e., the *temperature difference* between the sample and reference, $\Delta T_{DTA} = T_S - T_R$, against the investigated reaction rate, $d\alpha/dt$. The value of the extent of reaction, α, is then evaluated by simple peak area integration assuming the averaged values of extensive (α) and intensive (T) properties obtained from the sample specimen. It may be complicated by the inherent effect of heat inertia, $C_p(d\Delta T_{DTA}/dT)$, when the DTA peak background is not simply given by a linear interpolation [2,3].

A similarly derived DSC equation shows the direct relationship for the measured *compensation thermal flux*, ΔQ, supplied to both specimens under the conditions where the specimen difference ΔT_{DTA} serves only as a regulated quantity kept as close to zero as possible. Therefore during any DTA experiments the actual heating rate of the

sample is in reality changed [4] because of the DTA deflection due to heat release and/or absorption, which is also a direct measure of the deviation between the true and programmed (predetermined) temperatures (maintained by the reference). At the moment when a completely controlled thermal condition of the specimens is attained [3] the DTA peak would be diminished while that of DSC becomes more accurate. Both types of measurement provide a unique source of input data which is usually undervalued and underestimated for more sophisticated kinetic analysis.

Initially we should make clear that ordinary DTA can never satisfy all the demands arising from specific characteristics of the glassy state and the non-equilibrium nature of its investigation. Micro-DTA, where possible temperature gradients of microgram samples are maximally decreased, is an useful tool for a precise detection of characteristic temperatures while macro-DTA enables more effective measurement of integral changes needed in calorimetry. However, glassy samples of shapes like fibres or very thin metallic ribbons or even fine powders must be treated with increased attention as the process of sample pretreatment as well as filling a DTA cell can introduce not only additional interfaces and defects but also unpredictable mechanical tension and interactions with the sample holder surface all of which are sensitively detected and exhibited on thermometric recordings. Under limiting conditions, and particularly for a very small sample, it is then difficult to distinguish between effects caused by bulk and surface properties of a sample as well as by a self-catalyzing generation of heat. Consequently heat transfer from the reacting zone may become a rate-controlling process [3].

3. Thermophysics of vitrification and crystallization

Glasses (obtained by a suitable rapid cooling of melts) or *amorphous solids* (reached by an effective disordering process) are in a constrained (unstable) thermodynamic state [5] which tends to be transformed to the nearest, more stable state on reheating [2, 6]. The well-known dependence of a sample's extensive property on temperature can best illustrate the possible processes which can take place during changes of sample temperature [3]. A most normal plot was found in the form of H versus T which can be easily derived using an ordinary lever rule from a concentration section of a conventional phase diagram [7]. The temperature derivatives of this course ($\mathrm{d}\Delta H/\mathrm{d}T$) resembles the DTA–DSC traces each peak and/or step corresponding to the individual transformation exhibited by the step and/or break in the related H vs T plot.

3.1. *Fundamentals of glass-formation processes*

Fig. 1 illustrates possible ways of achieving a *non-crystalline* state. The latter can be either glass obtained in the classical way of liquid freeze-in via the metastable state of undercooled liquid (RC) or any other amorphous phase prepared by disintegration of crystalline solids (MD, upwards from solid to dotted line) or deposition from the gaseous state (VD, to thin sloped line). In the latter cases the characteristic region of

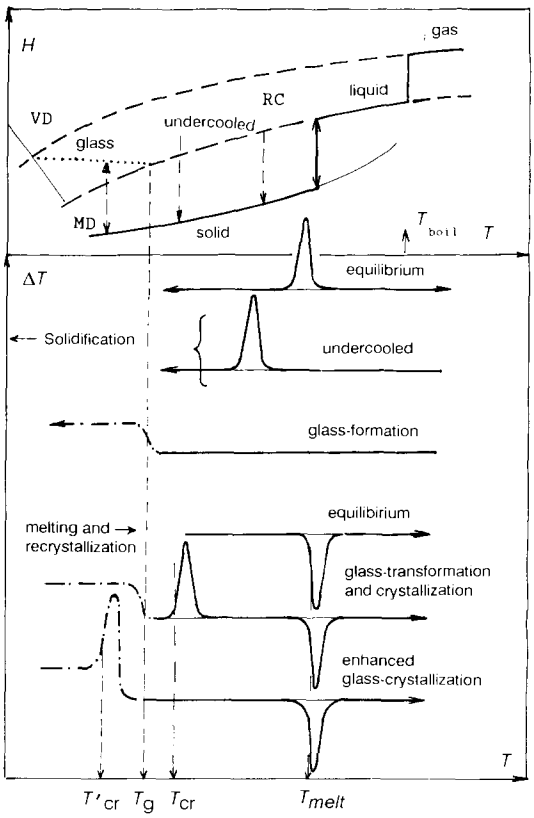

Fig. 1. Schematic diagram of enthalpy, H, versus temperature, T, and its derivative (ΔT) presented in the actual form which can be used to reconstruct the DTA–DSC recording. The solid, dashed and dotted lines indicate the stable, metastable and unstable (glassy) states. Rapid cooling of the melt (RC) can result in equilibrium or non-equilibrium solidification or glass-formation (T_g) which on reheating exhibits recrystallization. On the other hand an amorphous solid can be formed either by deposition of vapour (VD) against a cooled substrate (thin line) or the mechanical disintegration (MD) of the crystalline state (moving vertically to meet the dotted line). Reheating of such an amorphous solid often results in early crystallization which overlaps the T_g region.

glass-transformation is usually overlapped by early crystallization on heating which can be distinguished only by the baseline separation occurring due to the change of heat capacity. Such typical cases exist in oxide glasses but a better example can be found for non-crystalline chalcogenides prepared by various methods of disordering [8]. For most metallic glasses, however, there is negligible change of C_p between the glassy and crystalline states and thus the DTA–DSC baselines do not show the required displacement which even makes it difficult to locate T_g. It is worth noting that the entire glassy state [5] can further be classified according its origin, distinguishing liquid glassy crystals, etc. [9], characterised by their own glass-transformation regions.

3.2. Basic rules of relaxation and glass transformation

During heat treatment of an as-quenched glass relaxation processes can take place within the short and medium range ordering [10] to cover (i) *topological* short-range movement of constitutional species and relaxation of structural defects, (ii) *compositional* short-range rearrangements of the nearest neighbours where usually chemically similar elements can exchange their atomic positions and (iii) diffusional ordering connected again with structural defects and gradients created during quenching of real bodies [2, 10–13]. Such processes are typical during both the isothermal annealing and slow heating which occur below T_g and can consequently affect the glass transformation region as well as the medium-range ordering, possibly initiating segregation of clusters capable of easier nucleation. Characteristic types of T_g region during cooling and heating are illustrated at Fig. 2.

3.3. Crystallization of glasses

There are extensive sources of the basic theory for nucleation-growth controlled processes [14–17]; these form the framework of the resulting description of a centred process of overall crystallization. Schematically, see Fig. 3., the metastable glassy state (dotted) first undergoes glass transformation followed by separation of the closest crystalline phase usually metastable (dot-and-dashed). Consequent and/or overlapping T_g (I and II) indicate the possibility of two phase-separated glasses. If considering a more complex case, for example the existence of a second metastable phase, the sequences of processes became multiplied since the metastable phase is probably produced first to precipitate later into more stable phases. This can clearly give an idea of what kind of an equilibrium background [7] is to be considered for the overall crystallization. Thus the partial reaction steps experimentally observed as the individual peaks can be classified to fit the scheme chosen in accordance with the stable–metastable boundary lines in the given type of a phase diagram related to the sample composition [4].

4. Non-isothermal crystallization kinetics

4.1. Constitutive equations, derivation methods and applicability checking

The so-called *phenomenological description* of crystallization kinetics emerged as a separate category to enable utilization of thermoanalytically measured data on the mean and normalised extent of crystallization, α, for a simplified description of the nucleation-growth-controlled processes [3]. It is conventionally based on a physical–geometrical model, $f(\alpha)$, responsible for crystallization kinetics traditionally employing the classical Johnson–Mehl–Avrami–Yerofeeyev–Kolgomorov equation (abbreviated JMAYK) read as $-\ln(1-\alpha)=(k_T t)^r$. It follows that $f(\alpha)=(1-\alpha)(-\ln(1-\alpha))^p$ where $p=1-1/r$ [2, 3] has been derived, however, under *strict isothermal conditions*. Beside the standard requirements of random nucleation and

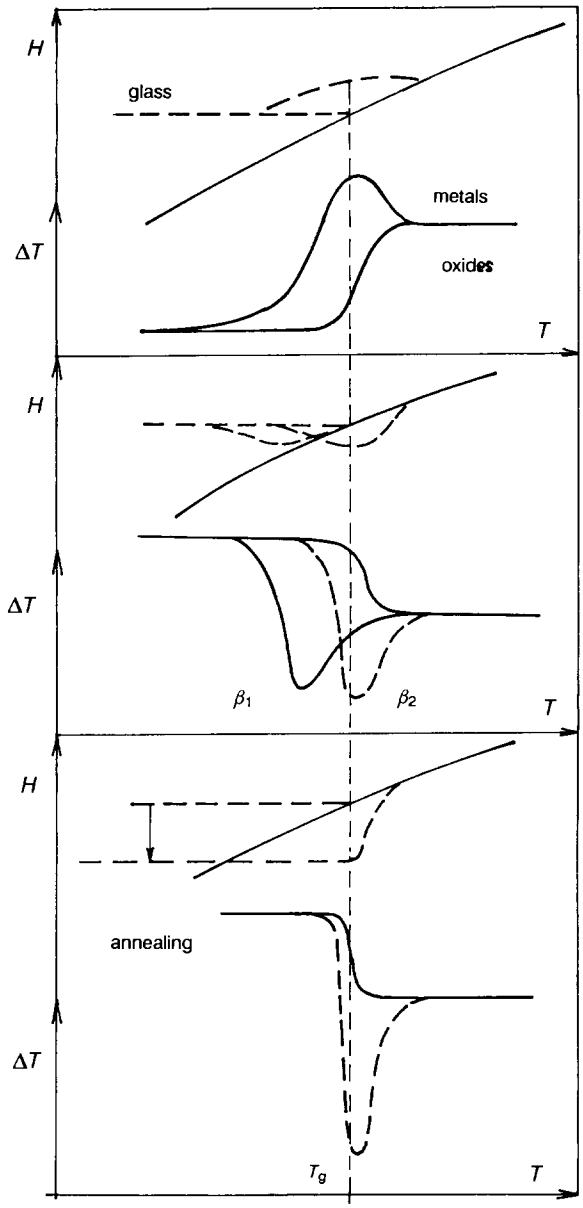

Fig. 2. Enlarged parts of a hypothetical glass transformation region (cf Fig. 1) shown for several characteristic cases such as cooling two different sorts of material (upper), reheating identical samples at two different heating rates (middle) and reheating after sample annealing (bottom).

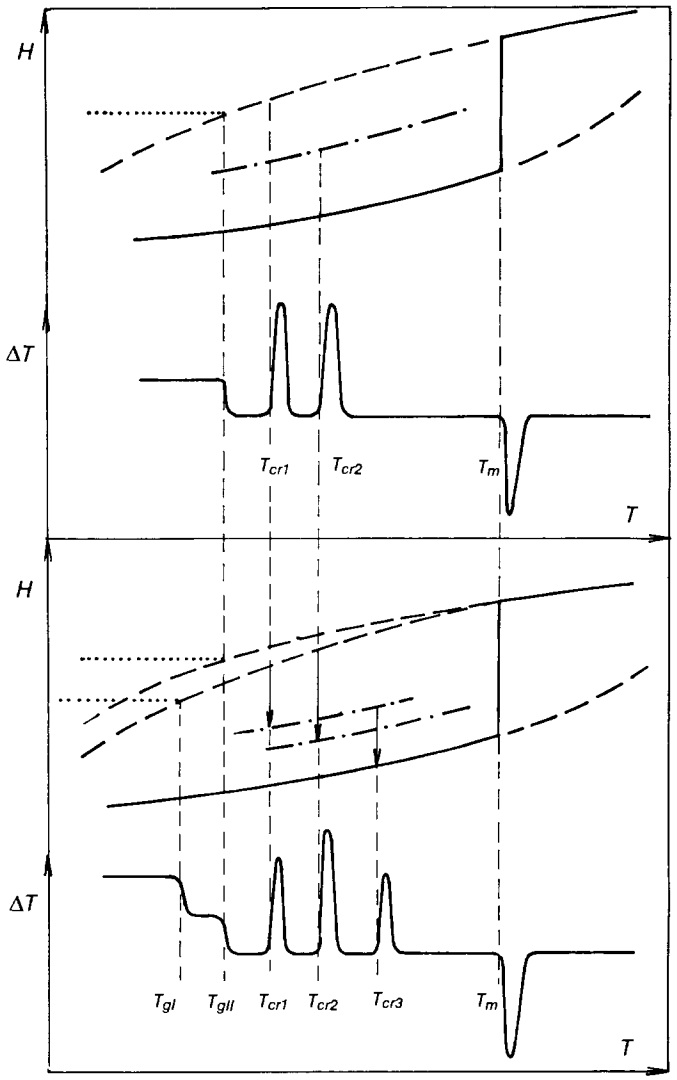

Fig. 3. Hypothetical crystallization of one metastable phase (T_{cr1}, dot-and-dashed line) or two metastable phases (T_{cr1}, T_{cr2}, bottom) including the possibility of two glasses (T_{gI}, T_{gII}), transformation as a possible result of preceding liquid–liquid phase separation.

consequent growth, the rate of which is temperature-but not time-dependent, the JMAYK equation is only valid at constant temperature. Some pecularities of non-isothermal kinetics and the general applicability of the JMAYK equation are thus worth reconsidering.

It must be reminded that the extent of crystallization, α, cannot be considered as a *state function* itself $\alpha \neq f_t(T,t)$ [3,7]. For the sake of simplicity the truly effective

constitutive equation in kinetics can thus be simplified to be valid for the two basic rates only, i.e., that of crystallization $d\alpha/dt = f_\alpha(\alpha, T)$ and of temperature change $dT/dt = f_T(\alpha, T)$. Therefore any additional term of the type $(d\alpha/dT)_t$ sometimes required to correct the non-isothermal rate in the fundamental Arrhenius equation [18,19] $d\alpha/dt = k_T f(\alpha)$ by the additional multiplying term $[1 + (T - T_0)E/RT^2]$ is unjustified [7] and incorrect [3]. The resultant *isokinetic* hypothesis is then accounted for in the construction of TTT and CT diagrams [2], also.

The true temperature-dependent intergration of the basic nucleation–growth equation yields very similar dependences [3,20] comparable to the classical JMAYK equation obtained under classical isothermal derivation. It effectively differs only by a constant in the preexponential factor depending on the numerical approximation employed during the integration [3]. This means that the standard form of the JMAYK equation can be used throughout non-isothermal treatments. Therefore a simple preliminary test of its applicability is recommendable. In particular, the value of the multiple $(d\alpha/dt)T$ can be used to check which maximum should be confined to the value 0.63 ± 0.01 [21]. Another handy test is the shape index, i.e., the ratio of intersections (b_1 and b_2) of the inflection slopes with the linearly interpolated peak baseline which should show a linear relationship [21] $\vartheta = b_1/b_2 = 0.52 + 0.916[(T_{i2}/T_{i1}) - 1]$ where T_i are respective inflection point temperatures.

This highly mechanistic picture of an idealized process of crystallization bears, however, a little correlation to morphological views and actual reaction mechanism [21,22]. If neither the $(d\alpha/dt)T$ value nor the shape index ϑ comply to JMAYK requirements we have to account for real shapes, anisotrophy, overlapping, etc., being usually forced to use a more flexible empirical kinetic model function usually based on two exponents (SB) instead the one (JMAYK) only.

4.2. *Apparent values of activation energies*

Conventional analysis of the basic JMAYK equation shows that the overall value of activation energies, E_{app}, usually evaluated from DTA–DSC measurements, can be roughly correlated on the basis of the partial energies of nucleation E_{nucl}, growth E_{gr} and diffusion E_{diff} [23]. It follows [24] that $E_{app} = (\upsilon E_{nucl} + \psi d E_{gr})/(\upsilon + \psi d)$ where the denominator equals the power exponent of the JMAYK equation, r, and the coefficients υ and d indicate the nucleation velocity and the growth dimensionality. The value of ψ corresponds to 1 or 1/2 for the movement of the growth front controlled by chemical boundary reaction or diffusion, respectively.

The value of E_{app} is easily determined from the classical Kissinger plot [3,4] of $\ln(\beta/T_p^2)$ versus $(-1/RT_p)$ for a series of the DTA–DSC peak apexes (T_a) at different heating rates (β) irrespective of the value of exponent r. Adopting the β-dependent concentration of nuclei Matusita and Sakka [25] proposed a modified equation of $\ln(\beta^{(r+d)}/T_a^2)$ versus $(-dE_{gr}/RT_a)$ applicable to the growth of bulk nuclei where the nuclei number is inversely proportional to the heating rate ($\upsilon \simeq 1$). This is limited, however, to such a crystallization where the nucleation and growth temperature regions are not overlapping. If $E_{nucl} = 0$ then E_{app} simplifies to the ratio $(dE_{gr} + 2[\upsilon + d - 1]RT_a)/(d + \upsilon)$ where $dE_{gr} \gg 2[r + d - 1]RT_a$. There are various

further explanations of the effective meaning which can be associated with the value of apparent activation energy [4, 20, 21, 26, 27].

4.3. *Effect of particle size*

In the case of surface-controlled crystallization the DTA exotherm is initiated at a lower temperature for the smaller particle size. In contrast the temperature region for the growth of bulk nuclei is independent of particle size. Thus for larger particles the absolute number of surface nuclei is smaller owing to the smaller relative surface area in the particle assembly resulting in predominant growth of bulk nuclei. With decreasing particle size the number of surface nuclei gradually increases, becoming responsible for the DTA exotherm. The particle-size-independent part of E_{app} can be explained on the basis of the nucleus formation energy being a function of the curved surface. Concave and convex curvature decreases or increases, respectively, the work of nucleus formation [24]. Extrapolation of E_{app} to the flat surface can be correlated with E_{gr}, $\upsilon = 1$ and $d = 3$, being typical for silica glasses. It, however, is often complicated by secondary nucleation at the reaction front exhibited by decreasing E_{app} with rising temperature for the various particle zones. The invariant part of E_{app} then falls between the microscopically observed values of E_{gr} and E_{nucl} the latter being frequently a characteristic value for a yet possible bulk nucleation for the boundary composition of a given glass.

Assuming that the as-quenched glass has a nuclei number equal to the sum of a constant number of quenched-in nuclei and that, depending on the consequent time-temperature heat treatment, the difference between the DTA–DSC apex temperatures for the as-quenched and nucleated glass ($T_a - T_a^0$) becomes proportional to the nuclei number formed during thermal treatment [26, 28]. A characteristic nucleation curve can then be obtained by plotting ($T_a - T_a^0$) against temperature [26] or even simply using only the DTA–DSC peak width at its half maximum [28].

For much less stable metallic glasses the situation becomes more complicated because simultaneous processes associated with the primary, secondary and eutectic crystallization often take place not far from each other's characteristic composition. Typically thin ribbons of iron-based glasses close to the critical content, x, of metalloids ($x_B + x_{Si} = 25\%$ with glass-forming limit $x_B \simeq 10\%$) usually exhibit two consecutive peaks. This is frequently explained by the formation of α-Fe embryos in the complex matrix containing quench-in sites followed by the formation of the metastable Fe_3Si-like compounds which probably catalyze heterogeneous nucleation of more stable compounds. Experimental curves are usually fitted by the classical JMAYK equation describing nucleation and three-dimensional growth. However, small additions of Cu and/or Nb cause the two DTA peaks to overlap each other, essentially decreasing inherent areas (the heat of crystallization is cut down to about one fourth) indicating probably the dopant surfactant effect directed on the critical work of nuclei formation due to the reduced surface energy. The resulting process of associated nanocrystal formation (fin-metals) [29–31] is thus different from the conventional nucleation–growth usually characterised by high $r(\geq 4)$. This is still far from being unambiguous and is often a matter of simplified hypotheses on grain growth. Nowadays *nanocrystallization* is thus another more specific case under increased attention becoming so

complicated to be explainable in terms of classical physical–geometrical theories. It is clear that a sort of fully *phenomenological* description could here be equally suitable for such a formal description, regardless of the entire mechanism of the reaction in question.

4.4. Phenomenological models in kinetics

There exist different phenomenological treatments, such as the geometric–probabilistic approach or a purely analytical description by the exponent containing the fraction $(a/x + b/x^2)^{-1}$. It enables continuous transfer from a quadratic to linear profile [3] making it possible to identify formally the changes of reaction mechanism by checking characteristics of the peak shape only. Nevertheless, for a general expression of heterogeneous kinetics a most useful approach seems to be the traditional type of a formal description based on an analytical model, $f(\alpha)$, regarded as a distorted case of the classical homogeneous-like description $(1-\alpha)^n$, where n is the so-called *reaction order*. A recently introduced function, $h(\alpha)$ [22], called the *accommodation function* (being put equal to either $(-\ln(1(1-\alpha))^p$ or α^m), expresses the discrepancy between the actual, $f(\alpha)$, and ideally simplified, $(1-\alpha)^n$ models. The simplest example of such an accommodation is the application of non-integral exponents (m, n, p) within the one- (JMAYK) or two- (SB) parametric function $f(\alpha)$, in order to match the best fitting of the functional dependences of an experimentally obtained kinetic curve. These non-integral kinetic exponents are then understood as related to the *fractal dimensions* [22]. From a kinetic point of view the interfacial area plays in crystallization kinetics the same role as that of concentration in homogeneous-like kinetics.

It is apparent that any specification of all (more complicated) processes in solid-state chemistry is difficult [32] to base unambiguously on physical–geometrical models although they have been a subject of the popular and widely reported evaluations [32–35]. As already mentioned it can be alternatively replaced by an empirical–analytical (SB) formula [3], $f(\alpha) = (1-\alpha)^n\alpha^m$, often called *Sestak–Berggren* equation [32, 34–36], which exhibits certain interrelation with the JMAYK equation, see Fig. 4. This can be found particularly serviceable in fitting the prolonged reaction tails due to the actual behaviour of real particles and can nicely match the particle non-sphericity, anisotropy, overlapping or other non-ideality [22].

It is worth mentioning that the typical kinetic data derived are strongly correlated with the Arrhenius equation, in the other words, a DTA–DSC peak can be interpreted within several kinetic models by simple variation of the activation energy E and preexponential factor A [36]. A correct treatment then requires an independent determination of E from multiple runs and its consequent use to analyse a single DTA–DSC peak in order to determine a more realistic kinetic model and preexponential factor [32, 34].

5. Crystallization of $ZnO–Al_2O_3–SiO_2$ glasses

An example of complex analysis of the crystallization processes is a complementary investigation of the above-mentioned system which is illustrated in Fig. 5. The upper

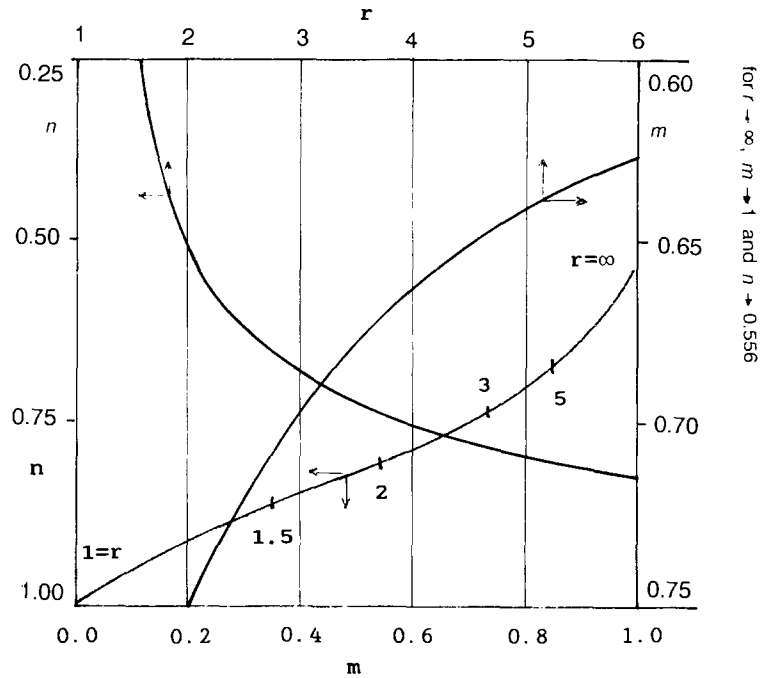

Fig. 4. This diagram demonstrates the relationship between the single exponent r of the JMAYK equation $-\ln(1-\alpha)=(k_T t)^r$ and the twin exponents n and m of the SB equation $(1-\alpha)^n\alpha^m$. Upper lines show the gradual development of both exponents m and n with r while the bottom curve illustrates a collective profile of n on m for increasing r.

part represents the standard data obtained by optical measurements by two-step method and the bottom part shows the associated DTA curves of variously treated samples.

For the powdered glass, where the surface crystallization of β-SiO_2 is dominant, the value of E_{app} was already reported [37] to correlate to the reciprocal of particle radius, indicating enhanced nuclei formation on a curved surface. Activation energy then changes as a function of the surface curvature and its extrapolation to the flat surface reaches $E_{app} = 50$ kcal comparable to $E_g = 66$ kcal for linear growth [37].

A more interesting case is certainly the bulk crystallization either spontaneous (gahnite and willemite) or catalysed (Zn-petalite) aimed at the preparation of low dilatation glass–ceramics. Assuming the crystal growth of Zn-petalite from both the constant number of nuclei (JMAYK, $r = 3$) and at the constant nucleation rate ($r = 4$) the theoretical DTA curve can be calculated and compared with the experimental one. For the instantaneous values of growth the best agreement was achieved for saturated nucleation based on the maximum nucleation rate. This is shown in Table 1 where the crystallization rates based on the optical and DTA measurements are compared, and agree within the order of magnitude. The apparent value of E derived from DTA traces

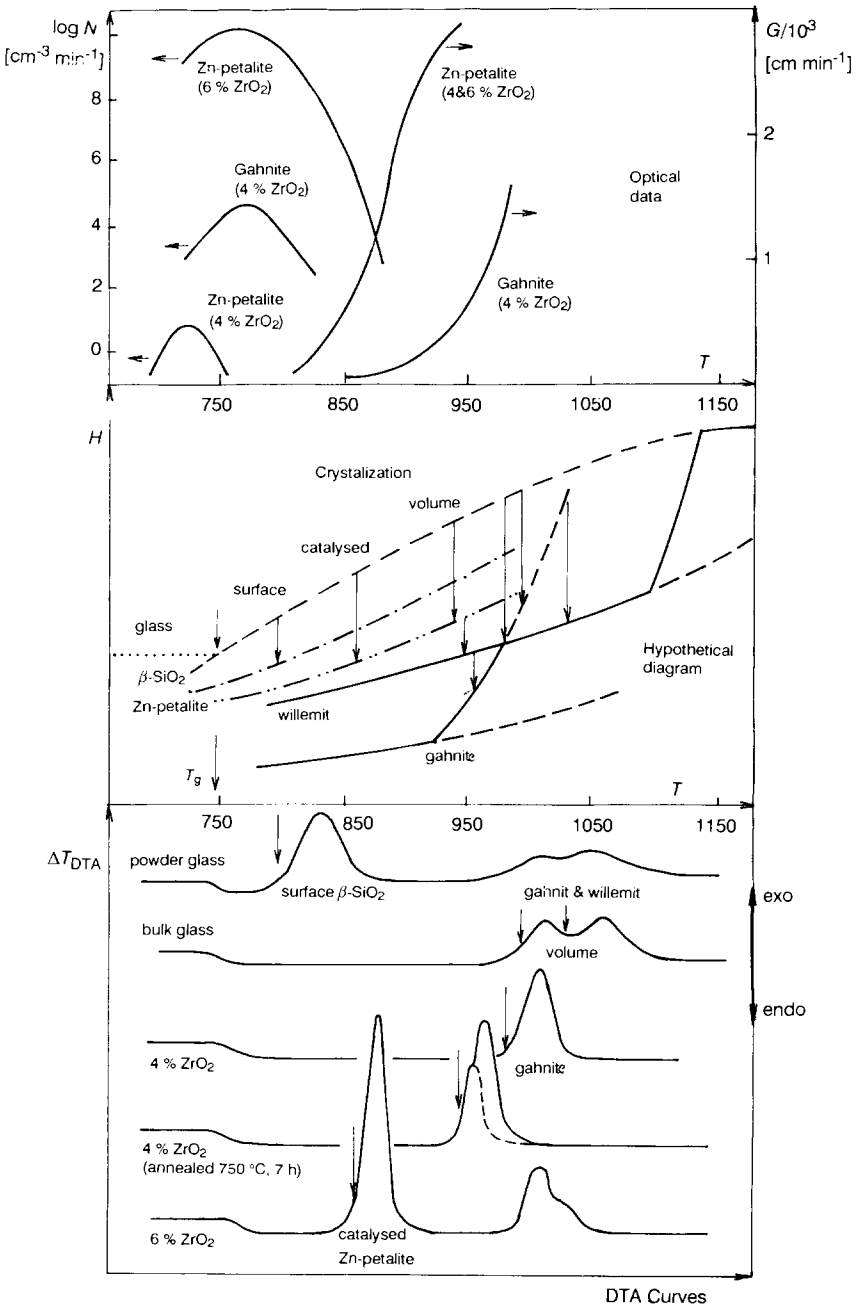

Fig. 5. Complex view to the crystallization behaviour of the $20ZnO–30Al_2O_3–70SiO_2$ glassy system showing its nucleation (N) and growth (G) data obtained by the classical two-step optical observation of growth (upper), schematic view of the enthaply versus temperature diagram exhibiting the presence of two metastable phases of β-quartz and Zn-petalite (middle) and respective DTA curves (bottom) obtained either on the powdered glass or on the bulk glass (cast directly into the DTA cell), in-weight about 200 mg, heating rate $10°C\,min^{-1}$ Netzsch apparatus with classical chart recording.

Table 1
Crystallization of Zn-petalite

Temperature/°C	Growth rate, G/(cm min^{-1})	Time of growth, t/min	$d\alpha/dT_{dir}$/(min^{-1})	$d\alpha/dT_{DTA}$/(min^{-1})
820	1.6×10^{-4}	2	1.6×10^{-2}	1×10^{-1}
830	1.9×10^{-4}	4	2.2×10^{-1}	4×10^{-1}
840	3.0×10^{-4}	6	2.9×10^{0}	1×10^{0}
850	4.6×10^{-4}	8	2.5×10^{1}	5×10^{0}
860	6.3×10^{-4}	10	1.2×10^{2}	8×10^{1}

$d\alpha/dT_{dir}$ was evaluated on basis of the JMAYK equation ($p = 2/3$) and optical data employing the growth rate in (cm min^{-1}) and saturation nucleation rate $N \simeq 5 \times 10^{10}$ (cm^{-3} min^{-1}), $d\alpha/dT_{DTA} = (K_{DTA}\Delta T + C_p\, d\Delta T/dT)/\Delta H$ where the apparatus constant K_{DTA} of the Netzsch instrument used was 5×10^2 (cal K^{-1} min^{-1}) at 850°C and the heat released $\Delta H \simeq 10$ cal.

($E_{app} \simeq 345$ kcal, see Table 2) also agrees with the sum of three E_{gr} ($\simeq 285$ kcal) indicating again the saturation of the sites capable of nucleation prior the growth process. Conventional analysis of the JMAYK exponent provided an exponent value close to three; thus both above-mentioned checks of the JMAYK validity were found to be positive. Simultaneously calculated [32, 34, 35] exponents of the SB equation give their respective values close to 3/4.

On the other hand the analogous analysis of gahnite crystallization shows the difference of about two orders of magnitude for both cases under calculation, see Table 3. Thus both tests for proving the validity of JMAYK also shows misfits. At the same time the E_{app} calculated from DTA is too low (about 130 kcal) to satisfy the triple value of responsible E_{gr} ($\simeq 75$ kcal) as shown in Table 2. Together with the delayed onset of the DTA peak and the shape of its accelerating part it clearly indicates a more complicated process than a single nucleation–growth event for gahnite. It is possibly affected by the ZrO_2-caused ordering which may affect prenucleus site formation [38–40]. The corresponding values of $r \simeq 3.3$ and $n \simeq 0.6$ and $m \simeq 0.7$ are again not

Table 2
Apparent kinetic data of the volume crystallization of $20ZnO–30Al_2O_3–70SiO_2$ glass doped with ZrO_2. Nucleation N in cm^{-3} min^{-1}, activation energy E in kcal

Nucleator content or treatment	Gahnite			Zn-petalite			E from DTA	
	N_{max}	E_{nucl}	E_{gr}	N_{max}	E_{nucl}	E_{gr}	Gahnite	Petalite
4% ZrO_2	6.4×10^4	115	75	5×10^0	45	95	130	–
Same, 7 h at 755°C	($\simeq 10^8$)[a]	–	–	($\simeq 10^7$)[a]	–	–	190	
6% ZrO_2	–	–	–	5×10^{10}	350	95	–	345

[a] Estimated from the DTA peak, other data from optical measurements, see Fig. 5.

Table 3
Crystallization of gahnite

Temperature/°C	Growth rate, G/(cm min^{-1})	Time of growth t/min	$d\alpha/dT_{dir}$/(min^{-1})	$d\alpha/dT_{DTA}$/(min^{-1})
820	$\simeq 10^{-6}$	28	$\simeq 10^{-4}$	$\simeq 10^{-2}$
960	9.6×10^{-5}	32	1.7×10^{-3}	6×10^{-1}
980	1.8×10^{-5}	36	1.6×10^{-2}	4×10^{0}
1000	2.2×10^{-5}	40	3.6×10^{-2}	9×10^{0}
1020	2.7×10^{-5}	44	1.0×10^{-1}	2×10^{1}
1040	2.9×10^{-5}	48	2.0×10^{-1}	5×10^{1}

$d\alpha/dT_{dir}$ was evaluated on basis of the YMAYK equation ($p = 2/3$) and optical data employing the growth rate in (cm min^{-1}) and saturation nucleation rate $N \simeq 6 \times 10^{4}$ (cm^{-3} min^{-1}), $d\alpha/dT_{DTA} = (K_{DTA}\Delta T + C_p\, d\Delta T/dT)/\Delta H$ where the apparatus constant K_{DTA} of the Netzsch instrument used was 9×10^{2} [cal K^{-1} min^{-1}] at 1000°C and the heat released $\Delta H \simeq 10$ cal.

characteristic enough for a single process to be simply understood without further complementary information.

Acknowledgement

The work was carried out under project no. A2010532 supported by the Academy of Sciences of the Czech Republic.

Deep thanks are due to Professor Z. Strnad of the Laboratory for Bioactive Glass–Ceramic Materials in Prague (LASAK) for kindly sharing optical measurements of the ZnO–Al_2O_3–SiO_2 system. Continuous cooperation in solving pecularities of non-isothermal kinetics is also appreciated, in particular mentioning Dr. J. Málek of the Laboratory for Solid-State Chemistry at the Pardubice University and Dr. N. Koga of the Chemistry Laboratory of Hiroshima University.

References

[1] J. Šesták, The Art and Horizon of Non-equilibrated and Disordered States and the New Phase Formation, in D. Uhlmann and W. Höland (Eds.), Proc. Kreidl's Symp. Glass Progress, Liechtenstein 1994, in press.
[2] J. Šesták, Glass: Phenomenology of Vitrification and Crystallization Processes, in Z. Chvoj, J. Sesták and A. Třiska (Eds.) Kinetic Phase Diagrams, Elsevier, Amsterdam 1991. p. 169.
[3] J. Šesták, Thermophysical Properties of Solids, Elsevier (Amsterdam) 1984.
[4] J. Šestak, Applicability of DTA and Kinetic Data Reliability of Non-isothermal Crystallization of Glasses, a Review, Thermochim. Acta, 98 (1986) 339.
[5] J. Šesták, Some Thermodynamic Aspects of Glassy State, Thermochim. Acta, 95 (1985) 459.
[6] J. Šesták, Thermal Treatment and Analysis in the Preparation and Investigation of Different Types of Glasses, J. Therm. Anal., 33 (1988) 789.
[7] P. Holba and J. Šesták, Kinetics of Solid State Reactions Studied at Increasing Temperature, Phys. Chem. Neue Folge, 80 (1971) 1.

[8] L. Červinka and A. Hrubý, Structure of amorphous and glassy sulphides, J. Non-Cryst. Solids, 48 (1982) 231.
[9] H. Suga, Calorimetric Study of Glassy Crystals, J. Therm. Anal., 42 (1994) 331; Thermochim. Acta 245 (1994) 69.
[10] J. Šestak, The Role of Thermal Annealing during Processing of Metallic Glasses, Thermochim. Acta, 110 (1987) 427.
[11] M. Lasocka, Reproducibility Effects within T_g Region, J. Mater. Sci. 15 (1980) 1283.
[12] E. Illeková, Generalised Model of Structural Relaxation of Metallic and Chalcogenide Glasses, Key Engineering Materials, 81–83 (1993) 541.
[13] J. Málek, Thermal Stability of Chalkogenide Glasses, J. Non-Cryst. Solids, 107 (1989) 323; J. Therm. Anal., 40 (1993) 159.
[14] M.C. Weinberg, Use of Saturation and Arrhenius Assumptions in the Interpretation of DTA–DSC Crystallization Experiments, Thermochim. Acta, 194 (1992) 93.
[15] E.D. Zanotto, Isothermal and Adiabatic Nucleation in Glasses, J. Non-Cryst. Solids, 89 (1987) 361.
[16] L. Granasy, Nucleation Theory for Diffuse Interfaces, Mater. Sci. Eng., A178 (1994) 121.
[17] P. Demo and Z. Kožíšek, Homogeneous Nucleation Process; Analytical Approach, Phys. Rev. B: 48 (1993) 362.
[18] E.A. Marseglia, Kinetic Theory of Crystallization of Amorphous Materials, J. Non-Cryst. Solids, 41 (1980) 31.
[19] H. Yinnon and D.R. Uhlmann, Application of TA Techniques to the Study of Crystallization Kinetics in Glass-Forming Liquids, J. Non-Cryst. Solids, 54 (1983) 253.
[20] T. Kemény and J. Šesták, Comparison of Equations Derived for Kinetic Evaluations under Isothermal and Non-Isothermal Conditions, Thermochim. Acta, 110 (1987) 113.
[21] J. Málek, Applicability of JMAYK Model in Thermal Analysis of the Crystallization Kinetics of Glasses, Thermochim. Acta, (in print 1995).
[22] J. Šesták, Diagnostic Limits of Phenomenological Kinetic Models when Introducing an Accommodation Function, J. Therm, Anal., 37 (1991) 111.
[23] J. Šesták, Application of DTA to the Study of Crystallization Kinetics of Iron Oxide-Containing Glasses, Phys. Chem. Glasses 15 (1974) 137.
[24] N. Koga and J. Šesták, Thermoanalytical Kinetics and Physico–geometry of the Non-Isothermal Crystallization of Glasses, Bol. Soc. Esp. Ceram. Vidrio, 31 (1992) 185.
[25] K. Matusita and S. Sakka, Kinetic Study of Non-Isothermal Crystallization of Glasses by DTA, Bull. Inst. Res. Kyoto Univ., 59 (1981) 159 (in Japanese).
[26] A. Marota, F. Branda and A. Buri, Study of Nucleation and Crystal Growth in Glasses by DTA, Thermochim. Acta, 46 (1981) 123; 85 (1985) 231; J. Mater. Sci., 16 (1981) 341.
[27] Q.C. Wu, M. Harmelin, J. Bigot and G. Martin, Determination of Activation Energies for Nucleation and Growth in Metallic Glasses, J. Mater. Sci., 21 (1986) 3581.
[28] C.S. Ray and D.E. Day, J. Am. Ceram. Sco., 73 (1990) 439; in M.C. Weinber (Ed.), Nucleation and Crystallization in Liquids and Glasses, Ceram. Trans., Am. Ceram. Soc. 1993, p. 207.
[29] N. Mingolo and O.E. Martinez, Kinetics of Glass Formation Induced by the Addition of Perturbing Particles. J. Non-Cryst. Solids, 146 (1992) 233.
[30] E. Illekova, K. Czomorova, F.A. Kunhast and J.M. Fiorani, Transformation Kinetics of FeCuNbSiB Ribbons to the Nanocrystalline State, Mater. Sci. Eng. A:, in print, 1995.
[31] L.C. Chen and F. Spaepen, Grain Growth in Microcrystalline Materials Studied by Calorimetry, Nanostructured Mater., 1 (1992) 59.
[32] J. Šesták, and J. Málek, Diagnostic Limits of Phenomenological Models of Heterogeneous Reactions and Thermal Analsysi Kinetics, Solid State Ionics 63–65 (1993) 245.
[33] S. Surinach, M.D. Baro, M.T. Clavaguera-Mora and N. Clavaguera, Kinetic Study of Isothermal and Continuous Heating Crystallization Alloy Glasses, J. Non-Cryst. Solids, 58 (1983) 209.
[34] J. Málek, Kinetic Analysis of Nonisothermal Data, Thermochim. Acta, 200 (1992) 257.
[35] J. Málek and J.P. Criado Empirical Kinetic Models in Thermal Analysis, Thermochim. Acta, 203 (1992) 25.
[36] N. Koga, Mutual Dependence of the Arrhenius Parameters Evaluated by TA Study of Solid-State Reactions: Kinetic Compensation Effect, Thermochim. Acta, 244 (1994) 1.

[37] Z. Strnad and J. Šesták, Surface Crystallization of $70SiO_2$–$30Al_2O_3$–$20ZnO$ Glasses, in Reactivity of Solids, (Proc. ICRS), Elsevier, Amsterdam, 1977, p. 410.
[38] J. Šesták and J. Šestáková, Thermodynamic and Kinetic View of Transformation Processes in Glasses, in Thermal Analysis (Proc. ICTA), Heyden, Tokyo/London, 1978, p. 222.
[39] N. Koga, J. Šesták and Z. Strnad. Crystallization Kinetics, in Soda-Lime –Silica System by DTA, Thermochim. Acta, 203 (1992) 361.
[40] Z. Kožíšek and P. Demo, Transient Kinetics of Binary Nucleation, J. Cryst. Growth, 132 (1993) 491.
[41] A. Dobrewa and I. Gutzow, Kinetics of Non-Isothermal Overall Crystallization in Polymer Melts, Cryst. Res. Tech., 26 (1991) 863; J. Appl. Polym. Sci., 48 (1991) 473.
[42] M.C. Weinberg, Analysis of Nonisothermal Thermoanalytical Crystallization Experiments J. Non-Cryst. Solids, 127 (1991) 151.